

Design and Analysis of Plastic Pocket Automotive

Cigelouis

Department of mechanical, VIVA institute, Mumbai University, Mumbai

Email: cige.louis86@gmail.com

Abstract—Plastics structures often undergo permanent deformations at support location such as ribs, bosses etc. Remaining area of part barely takes loads as compared to these stiffened locations. Hence, achieving optimum design through FEA helps in reducing number of prototypes required for testing. CAD designing of plastic component will be done using CATIA V5 software. Discretization (Meshing) will be done with help of tetrahedron/hexahedron elements using Ansys Workbench. Nonlinear simulation will be carried out using variation in stiffening ribs. Final design will be manufactured using 3D printing technology. Specimen will be tested on UTM for Denting (Compression) test. Comparative analysis of Reaction forces will be made between simulation and experimental results. Results and conclusions will be drawn. Suitable future scope will be suggested.

Keywords— Plastic Structures, FEA, CATIA, UTM, Reaction forces

I. INTRODUCTION

The concept of 3D printing manufacturing process covers a variety of processes in which material is joined or solidified under computer control to create 3D object, with material being added together (such as liquid molecules or powder grains being fused together), typically layer by layer. In the 1990s, three dimension printing techniques were considered suitable only for the construction of functional or aesthetical prototypes and a more correct term was prototyping. Nowadays, the correctness, repeatability and material range have increased to the point that some 3D printing processes are considered viable as an industrial production technology, whereby the term additive manufacturing can be used equally with 3D printing. One of the key advantages of three dimension printing is the ability to produce very complex shapes or geometries, and a prerequisite for producing any three dimension printed part is a digital three dimension model or a CAD file.

The most commonly used 3D Printing process is a material extrusion approach called fused deposition modelling (FDM). Metal Powder bed fusion has been gaining prominence lately during the immense function of metal parts in the 3D printing industry. In 3D Printing, a three-dimensional object is built from a computer-aided design (CAD) model, usually by successively adding material layer by layer, unlike the current machining process, where material is removed from a stock item, or the casting and forging processes which date to antiquity.

3D printing technology basically referred to a process that deposits a binder material onto a powder bed with inkjet printer heads coat by coat. Now days, the term is being used in popular vernacular to encompass a wider collection of additive manufacturing techniques. United States and global technical standards use the official term *additive manufacturing* for this broader sense.

General Principles:

Modelling

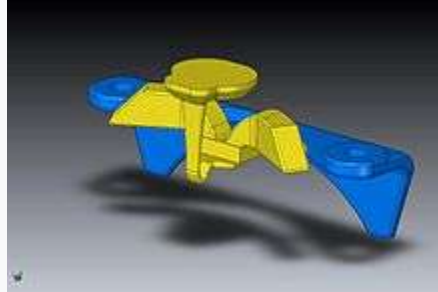


FIGURE 1:CAD model used for 3D printing



FIGURE 2:3D models can be generated from 2D pictures taken at a 3D photo booth.

printable models of three dimension may be created with a computer-aided design (CAD) package, via a 3D scanner, or by a plain digital camera and photogrammetric software. 3D printed models created with CAD result in reduced errors and can be corrected before printing, allowing verification in the design of the object before it is printed. The manual modeling process of preparing geometric data for 3D computer graphics is similar to plastic arts such as sculpting. 3D scanning is a process of collecting digital data on the shape and appearance of a real object, creating a digital model based on it.

CAD models can be saved in the stereo lithography file format (STL), a de facto CAD file format for additive manufacturing that stores data based on triangulations of the surface of CAD models. STL is not tailored for additive manufacturing because it generates large file sizes of topology optimized parts and lattice structures due to the large number of surfaces involved. A newer CAD file format, the Additive Manufacturing File format (AMF) was introduced in 2011 to solve this problem. It stores information using curved triangulations.

Printing

Before printing a 3D model from an STL file, it must first be examined for errors. Most CAD applications produce errors in output STL files,[29][30] of the following types:

1. holes;
2. faces normals;
3. self-intersections;
4. noise shells;

5. manifold errors.

A step in the STL generation known as "repair" fixes such problems in the original model. Generally STLs that have been produced from a model obtained through 3D scanning often have more of these errors. This is due to how 3D scanning works-as it is often by point to point acquisition, 3D reconstruction will include errors in most cases.

Once completed, the STL file needs to be processed by a piece of software called a "slicer," which converts the model into a series of thin layers and produces a G-code file containing instructions tailored to a specific type of 3D printer (FDM printers). This G-code file can then be printed with 3D printing client software (which loads the G-code, and uses it to instruct the 3D printer during the 3D printing process).

Printer resolution describes layer thickness and X-Y resolution in dots per inch (dpi) or micrometers (μm). Typical layer thickness is around $100\ \mu\text{m}$ (250 DPI), although some machines can print layers as thin as $16\ \mu\text{m}$ (1,600 DPI). X-Y resolution is comparable to that of laser printers. The particles (3D dots) are around 50 to $100\ \mu\text{m}$ (510 to 250 DPI) in diameter.^[citation needed] For that printer resolution, specifying a mesh resolution of 0.01–0.03 mm and a chord length ≤ 0.016 mm generate an optimal STL output file for a given model input file. Specifying higher resolution results in larger files without increase in print quality.

II. LITERATURE REVIEW

Samy J. Ebeidet al. Carbon Black filled Acrylonitrile Butadiene Styrene (ABS) was used to prepare a polymer composite by Fused Deposition Modeling (FDM) technology. The effect of printing setup on the strain sensing behavior of the composite was investigated, targeting the fabrication of a functionalized composite that is able to detect stress or strain changes in engineering members. Experimental work revealed that internal stresses can be detected based on monitoring the change in resistance as a response to strain. Measurements across sample thickness were found to be most suitable for making general statements about the resistivity of the samples. Hereby, the resistance depends on the intrinsic and the process specific properties of the material. The printing setup was systematically varied in terms of raster angle and gap width. to yield the most sensitive constellation for conductivity. The use of a negative gap between the individual rasters in combination with a raster angle of $\pm 45^\circ$ was observed to have a positive influence on intensifying the detected signals, making this constellation most sensible for strain sensing applications. Hence, the intrinsic properties of material were enhanced by the adequate selection of processing parameters. This study shows that the functionalized composite can be used as a strain sensor as for health monitoring purposes, to give an example.[1].

B. Read et al. Computer methods based on finite element analysis are able to predict the performance of plastics under impact loading. Although the accuracy of results depends on the model used to describe the deformation behaviour of the polymer, whichever model is used, the analysis requires stress/strain data over a wide range of strain rate. These data are most conveniently measured in tension, but procedures are currently not available for determining results at high strain rates. ISO standards for tensile property measurement are applicable for strain rates up to around 0.1 s⁻¹. To simulate behaviour under impact, data are required at rates that are 3 or 4 orders of magnitude higher than this. For accurate data acquisition at these higher rates, attention needs to be paid to apparatus design in order to minimise contributions from transient forces arising from resonances and the propagation of shock waves in the apparatus. In addition, procedures and extensometers are not routinely available for determining strains at the higher rates of deformation. This paper illustrates the acquisition of data over a wide range of strain rates through a combination of measurements at low and moderate strain rates with extrapolation of these data to higher rates. In order to maximise accuracy at moderate strain rates, suitable designs need to be selected for the transducers, the test specimen geometry and the test assembly. Extrapolation is achieved by the use of mathematical functions to model the stress/strain curves and their rate dependence. Reference is also made to the development of a new materials model for describing the deformation behavior of toughened plastics at large strains. Δ 2001 NPL. Published by Elsevier Science Ltd. All rights reserved.[2].

C. Dumaset al. Multiaxial fatigue behavior of polypropylene pipes is investigated under tension and torsion loading with or without mean stress. Fatigue limit is experimentally determined and compared to self-heating curve method. A multiaxial fatigue criterion is proposed and shows that the fatigue behavior of this semi-crystalline polymer seems to be governed by the von Mises maximum stress. [3].

TiantianLi,etalWe combine 3D printing technique, numerical analysis, and experiments to design a new class of sandwich composites that exhibit various bending behaviors. These programmed sandwich structures contain 3D printed core materials

with truss, conventional honeycomb, and re-entrant honeycomb topologies. Three-point bending tests are performed to investigate the bending behavior of these sandwich composites with two types of carbon fiber reinforced polymer face sheets. Under bending deformation, sandwich composites with truss core materials provide highest flexural stiffness and strength that are desirable in structural components. The sandwich composites with re-entrant honeycomb core exhibit a sequential snap-through instability which significantly enhances the energy absorption abilities. Our experimental and numerical results indicate that architected core structures can be utilized to tailor the bending properties as well as failure mechanisms. These findings offer new insights into the study of nonlinear mechanical response of sandwich structures, which can benefit a wide range of industries and applications[4].

TiantianLi, et al. Interpenetrating phase composite (IPC), also known as co-continuous composite, is one type of material that exhibits an unusual combination of high stiffness, strength, energy absorption, and damage tolerance. Here we experimentally demonstrate that IPCs fabricated by 3D printing technique with rationally designed architectures can exhibit a fracture toughness 16 times higher than that of conventionally structured composites. The toughening mechanisms arise from the crack-bridging, process zone formation and crack deflection, which are intrinsically controlled by the rationally designed interpenetrating architectures. We further show that the prominently enhanced fracture toughness in the architected IPCs can be tuned by tailoring the stiffness contrasts between the two compositions. The findings presented here not only quantify the fracture behavior of complex architected IPCs but also demonstrate the potential to achieve tailor able mechanical properties through the integrative rational design and the state-of-the-art advanced manufacturing technique.[5].

III. PROBLEM STATEMENT

Plastics structures often undergo permanent deformations at support location such as ribs, bosses etc. Remaining area of part barely takes loads as compared to these stiffened locations. Hence, achieving optimum design through FEA helps in reducing number of prototypes required for testing.

IV. OBJECTIVES

1. To prepare CAD design using Catia V5
2. To design various models with variation in rib design
3. To select suitable material available in 3D printers for manufacturing
4. To perform Meshing and Nonlinear (Material and Contact) Analysis
5. To 3D print single specimen using suitable printer for Testing purpose
6. To perform Compression test on UTM for extracting Reaction forces vs deflection plots
7. To make comparative analysis between FEA and Experimental results
8. Results & Conclusion

V. METHODOLOGY

Step 1: - I started the work of this project with literature survey. I gathered many research papers which are relevant to this topic. After going through these papers, I learnt about the Plastic Component.

Step 2: - After learning the concept, the 3 D Model and drafting will be done with the help of CATIA software.

Step 3: - The experimental testing was carried out after making the assembly of the project.

Step 4: - After making the testing the result & conclusion was drawn.

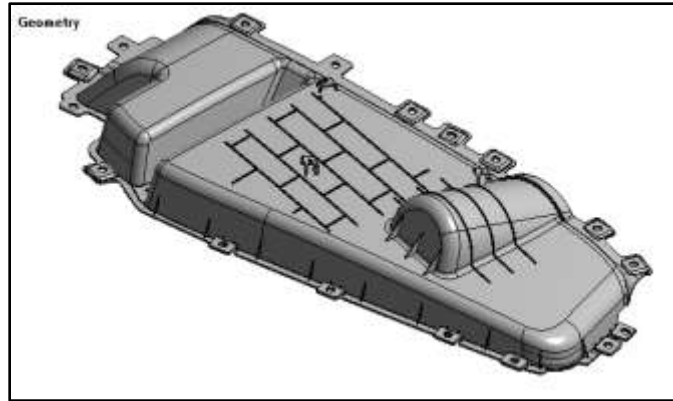


FIGURE 3: Cad Model Of Plastic Pocket Automotive With Brick Stiffeners

Material properties of plastic pocket

Properties of Outline Row 3: POLYPROPYLENE			
	A	B	C
1	Property	Value	Unit
2	Material Field Variables	Table	
3	Isotropic Elasticity		
4	Derive from	Young's Modulu...	
5	Young's Modulus	1500	MPa
6	Poisson's Ratio	0.3	
7	Bulk Modulus	1250	MPa
8	Shear Modulus	576.92	MPa

MESH

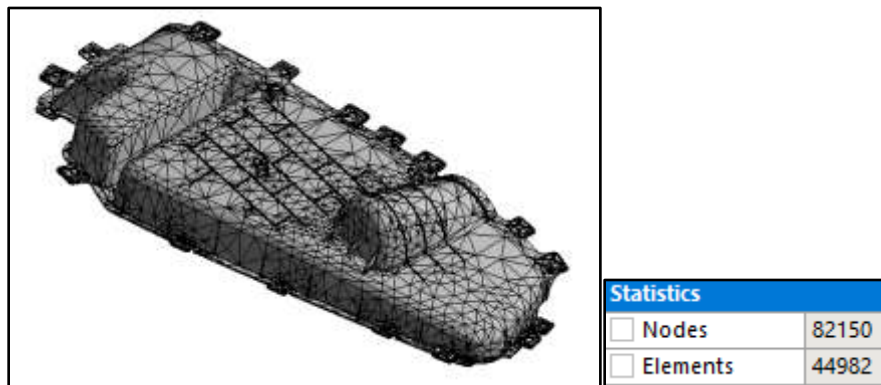


FIGURE 4: Meshing Of Plastic Pocket Automotive With Brick Stiffeners

BOUNDARY CONDITION

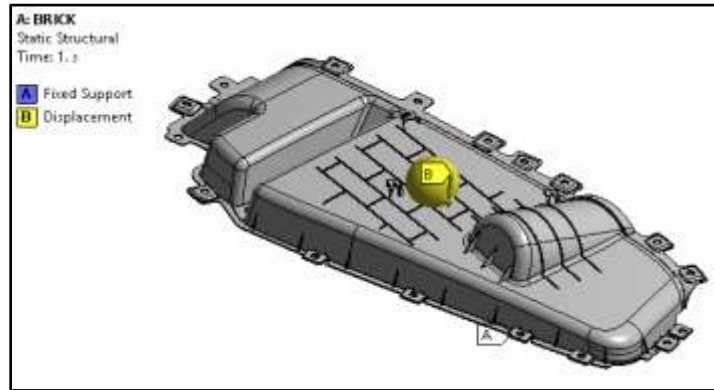


FIGURE 5: Boundary condition Of Plastic Pocket Automotive With Brick Stiffeners

For boundary condition for model bottom surface of plastic pocket is fix and steel ball is applied on upper side

TOTAL DEFORMATION

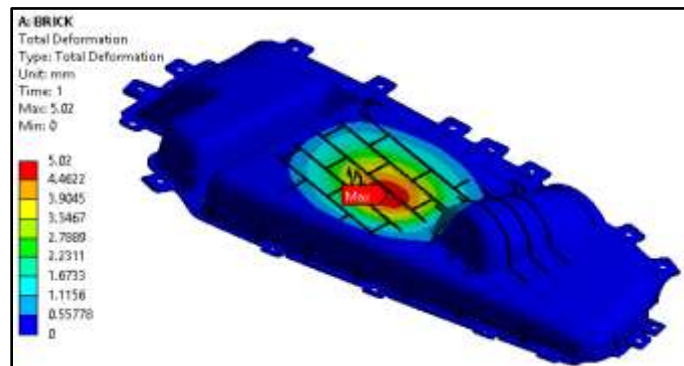


FIGURE 6: Total Deformation Of Plastic Pocket Automotive With Brick Stiffeners.

maximum deformation of plastic pocket Automotive With Brick Stiffeners is 5.02 mm.

EQUIVALENT STRESS

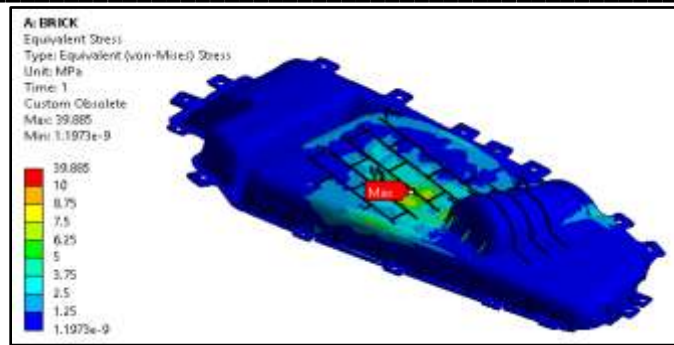


FIGURE 7:Equivalent Stress Of Plastic Pocket Automotive With Brick Stiffeners.

maximum Equivalent Stress of plastic pocket Automotive With Brick Stiffeners is 39.885 MPa

FORCE REACTION

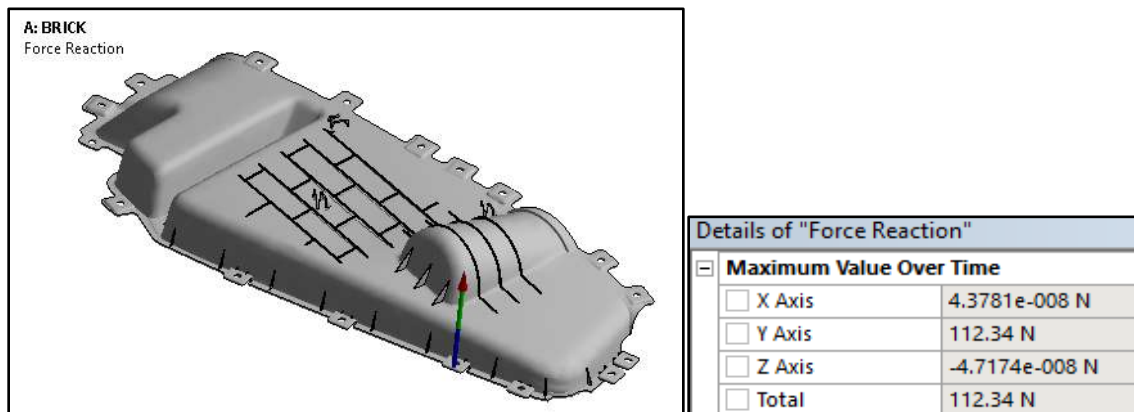


FIGURE 8:Force Reaction Of Plastic Pocket Automotive With Brick Stiffeners.

Force Reaction Of Plastic Pocket Automotive With Brick Stiffeners is 112.34N

CYLINDRICAL STIFFENERS

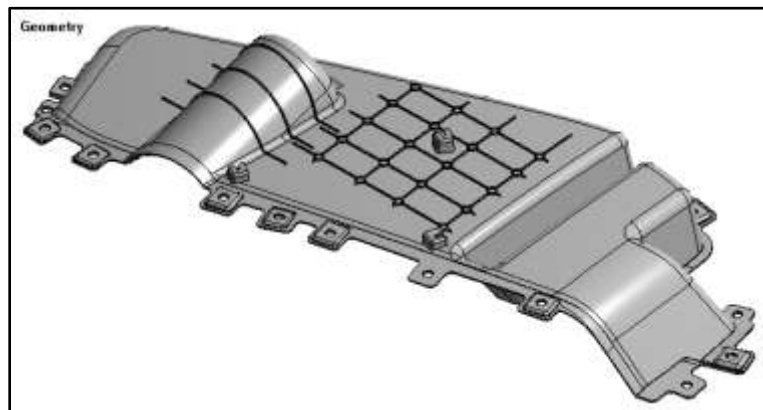


FIGURE 9: Cad Model Of Plastic Pocket Automotive With Cylindrical Stiffeners

VI.RESULT

	Total Deformation	Equivalent Stress	Force Reaction
With Brick Stiffeners	5.02mm	39.885MPa	112.34N
With Cylindrical Stiffeners	5.044mm	42.621MPa	105.67N

VII.CONCLUSION

1. Maximum deformation of plastic pocket Automotive With Brick Stiffeners is 5.02 mm
2. Total Deformation Of Plastic Pocket Automotive With Cylindrical Stiffeners is 5.044mm
3. Reaction force of plastic pocket Automotive With Brick Stiffeners has greater force than Plastic Pocket Automotive With Cylindrical Stiffeners. Hence conclude that strength of Brick Stiffeners better than Cylindrical Stiffeners.
4. Force reaction Of Plastic Pocket Automotive With Cylindrical Stiffeners is 105.67N.

REFERENCES

1. D. KoteswaraRao, Tarapada Roy., 2016, *Vibration Analysis of Functionally Graded Rotating Shaft System*, Journal of Procedia Engineering, Vol.144, pp. 775- 780.
2. DebabrataGayen, DebabrataChakraborty., 2016, *Variation of Local Flexibility Coefficients of Functionally Graded Cracked Shaft*, Journal of Procedia Engineering, Vol.144, pp. 1443-1450.
3. H. Bayrakceken, S. Tasgetiren, I. Yavuz., 2007, *Two cases of failure in the power transmission system on vehicles: A universal joint yoke and a drive shaft*, Journal of Engineering Failure Analysis, Vol. 14, pp.716-724.
4. Osman Asi., 2006, *Fatigue failure of a rear axle shaft of an automobile*, Journal of Engineering Failure Analysis, Vol.13, pp. 1293 - 1302.
5. H. Bayrakceken., 2006, *Failure analysis of an automobile differential pinion shaft*, Journal of Engineering Failure Analysis, Vol.13, pp. 1422 – 1428.
6. J Vogwell., 1998, *Analysis of a vehicle wheel shaft failure*, Journal of Engineering Failure Analysis, Vol.5, No. 4. Pp. 271-277.
7. G.K. Nanaware, M.J. Pable., 2003, *Failures of rear axle shafts of 575 DI tractors*, Journal of Engineering Failure Analysis, Vol. 10, pp.719-724.
8. S.K. Bhaumik, R. Rangaraju, M.A. Parameswara, M.A. Venkataswamy, T.A. Bhaskaran, R.V. Krishnan., 2002, *Fatigue failure of a hollow power transmission shaft*, Journal of Engineering Failure Analysis, Vol.9. pp. 457 - 467.
9. F. Jimenez Espadafor, J. Becerra Villanueva, M. Torres Garcia., 2009, *Analysis of a diesel generator crankshaft failure*, Journal of Engineering Failure Analysis, Vol.16. pp. 2333 - 2341.
10. V. Veloso, H.S. Magalhaes, G.I. Bicalho, E.S. Palma., 2009, *Failure investigation and stress analysis of a longitudinal stringer of an automobile chassis*, Journal of Engineering Failure Analysis, Vol.16. pp. 1696 - 1702.
11. YiminShao, JingLiu, Chris K. Mechefske., 2011, *Drive axle housing failure analysis of a mining dump truck based on the load spectrum*, Journal of Engineering Failure Analysis, Vol.18. pp. 1049 - 1057.
12. M.A. Badie, E. Mahdi, A.M.S. Hamouda., 2011. *An investigation into hybrid carbon/glass fiber reinforced epoxy composite automotive drive shaft*, Journal of Materials and Design, Vol.32. pp. 1485 - 1500.